Monoisocyanide Adducts of Ditungsten Hexaalkoxides. Synthetic, Structural, and Theoretical Investigations into the Nature of C=N Bond Order Reduction

M. H. Chisholm,* D. L. Clark, D. Ho, and J. C. Huffman

Department of Chemistry and Molecular Structure Center, Indiana University, Bloomington, Indiana 47405

Received December 23, 1986

Addition of xylyl and *tert*-butyl isocyanide (1 equiv) to $W_2(O\text{-}t\text{-}Bu)_6$ and $W_2(O\text{-}i\text{-}Pr)_6(py)_2$ in hydrocarbon solvents has allowed for the isolation of the 1:1 adducts $W_2(O\text{-}t\text{-}Bu)_6(CNR)$ and $W_2(O\text{-}i\text{-}Pr)_6(py)(CNR)$. The compounds where R = xylyl have been structurally characterized. In both there are W–W distances of ca. 2.52 Å and bent μ-CNAr ligands, C–N–C = ca. 130°, with the CNC plane being aligned along the M–M axis. Variable-temperature NMR studies show that the compounds are fluxional in solution, and low-temperature spectra show that inversion at the isocyanide nitrogen has not been frozen out. The ability of the isopropoxy compound to coordinate one pyridine molecule can be understood in terms of steric pressure at the W_2 center. These synthetic and structural findings are compared to related carbonylations which yield $W_2(O\text{-}t\text{-}Bu)_6(\mu\text{-}CO)$ and $W_2(O\text{-}i\text{-}Pr)_6(py)_2(\mu\text{-}CO)$. The bonding in the $W_2(\mu\text{-}CX)$-containing compounds is compared with the aid of computations employing the method of Fenske and Hall, where X = O, NH, and NMe. The computational results provide a relationale for (i) the observed C–N–C bending of the isocyanide ligand and (ii) the asymmetric nature of the W_2–μ-C bonds and a direct comparison of bridging CO and isocyanide ligands in structurally identical environments. Crystal data: (i) for $W_2(O\text{-}t\text{-}Bu)_6(CNxylyl)$ at −158 °C, a = 18.768 (5) Å, b = 23.566 (8) Å, c = 17.311 (6) Å, Z = 8, d_{calcd} = 1.63 g cm^{-3}, and space group *Pbca*; (ii) for $W_2(O\text{-}i\text{-}Pr)_6(py)(CNxylyl)$ at −155 °C: a = 9.880 (3) Å, b = 19.071 (6) Å, c = 19.903 (7) Å, β = 104.05 (1)°, Z = 4, d_{calcd} = 1.70 g cm^{-3}, and space group $P2_1/n$.

Introduction

In a previous paper, we described the reactions of $M_2(OR)_6(M{\equiv}M)$ compounds with alkyl and aryl isocyanides that lead to the cleavage of the metal–metal triple bond.[1] In the case of $Mo_2(O\text{-}t\text{-}Bu)_6$, isolation of $Mo(O\text{-}t\text{-}Bu)_4$ and $Mo(CNR)_7^{2+}$ suggested a parallel reactivity to that observed for the analogous carbonylation reactions that produce $Mo(O\text{-}t\text{-}Bu)_4$ and $Mo(CO)_6$.[2] Although detailed studies of the carbonylation reactions of $M_2(OR)_6$ (M = Mo, W) have demonstrated that these reactions proceed through intermediates of formula $M_2(OR)_6(\mu\text{-}CO)$,[3,4] no corresponding $M_2(OR)_6(\mu\text{-}CNR)$ compounds were isolated. Most of our previous work on isocyanide reactions centered around the chemistry of dimolybdenum species. However, our recent theoretical and spectroscopic studies on $M_2(OR)_6(\mu\text{-}CO)$ compounds of Mo and W emphasized the greater reducing strength and hence greater π backbonding for W relative to Mo analogues based on calculated orbital occupations of the CO ligand π^* orbitals.[5] This latter observation generated a renewed interest in the possible isolation of a compound of formula $M_2(OR)_6(\mu\text{-}CNR)$ by taking advantage of the greater reducing strength of the $(W{\equiv}W)^{6+}$ unit. We report here our successful synthesis and characterization of compounds of formula $W_2(OR)_6L_n(\mu\text{-}CNR')$ (R = *t*-Bu, *i*-Pr; R′ = xylyl, *t*-Bu; L = py; n = 0 or 1).

Results and Discussion

Syntheses and Physicochemical Properties. Hydrocarbon solutions of $W_2(O\text{-}t\text{-}Bu)_6$ react rapidly with 1 equiv of alkyl or aryl isocyanide ligands at 0 °C. When the solutions were cooled to ca. −15 °C, dark brown or dark green crystalline compounds $W_2(O\text{-}t\text{-}Bu)_6(\mu\text{-}CNR)$ were obtained in close to 60% yield for R = xylyl (xylyl = 2,6-dimethylphenyl) and *t*-Bu, respectively, as outlined in eq 1. The reaction conditions appear to be more sensitive

$$W_2(O\text{-}t\text{-}Bu)_6 + CNR \xrightarrow[0\ °C]{\text{toluene}} W_2(O\text{-}t\text{-}Bu)_6(\mu\text{-}CNR) \quad (1)$$

for alkyl than aryl isocyanide ligands. ^{1}H NMR spectra of the products obtained by removal of the reaction solvents in vacuo reveal that formation of $W_2(O\text{-}t\text{-}Bu)_6(\mu\text{-}CNR)$ is virtually quantitative when R = xylyl, whereas the products are contaminated with an as yet unidentified impurity when R = *t*-Bu.

For the carbonylation reactions of $M_2(OR)_6$ compounds, it has been shown that the donor ligands L in $M_2(OR)_6L_2(\mu\text{-}CO)$ compounds block further reaction with CO. The M–M bond rupture involves CO attack on $M_2(OR)_6(\mu\text{-}CO)$ or $M_2(OR)_6L(\mu\text{-}CO)$.[3] In an attempt to inhibit M–M bond cleavage and isolate products of less sterically demanding alkoxide ligands, an attempt was made to isolate compounds of formula $W_2(O\text{-}i\text{-}Pr)_6L_2(\mu\text{-}CNR)$. The isolation of a Lewis base adduct has thus far only been fruitful in the case of xylyl isocyanide. Hydrocarbon solutions of $W_2(O\text{-}i\text{-}Pr)_6(py)_2$ react rapidly with xylyl isocyanide at 0 °C to afford dark brown solutions. Cooling the solution to −15 °C produced a brown oily substance which resisted crystallization, presumably due to the presence of liberated pyridine. Removal of the reaction solvents and drying the solids in vacuo to remove free pyridine, followed by recrystallization from hexane, allowed for the isolation of dark brown crystals of $W_2(O\text{-}i\text{-}Pr)_6(py)(\mu\text{-}CNxylyl)$ in approximately 60% yield according to eq 2.

$$W_2(O\text{-}i\text{-}Pr)_6(py)_2 + CNxylyl \xrightarrow[0\ °C]{\text{toluene}} W_2(O\text{-}i\text{-}Pr)_6(py)(\mu\text{-}CNxylyl) + py \quad (2)$$

Solid-State and Molecular Structures. $W_2(O\text{-}t\text{-}Bu)_6(\mu\text{-}CNxylyl)$. Atomic positional parameters are given

(1) Chisholm, M. H.; Corning, J. F.; Folting, K.; Huffman, J. C.; Ratermann, A. L.; Rothwell, I. P.; Streib, W. E. *Inorg. Chem.* **1984**, *23*, 1037.
(2) Chisholm, M. H.; Cotton, F. A.; Extine, M. W.; Kelly, R. L. *J. Am. Chem. Soc.* **1979**, *101*, 7645.
(3) Chisholm, M. H.; Huffman, J. C.; Leonelli, J.; Rothwell, I. P. *J. Am. Chem. Soc.* **1982**, *104*, 7030.
(4) Chisholm, M. H.; Hoffman, D. M.; Huffman, J. C. *Organometallics* **1985**, *4*, 986.
(5) Blower, P. J.; Chisholm, M. H.; Clark, D. L.; Eichhorn, B. W. *Organometallics* **1986**, *5*, 2125.

0276-7333/87/2306-1532$01.50/0

Table I. Fractional Coordinates and Isotropic Thermal Parameters for the $W_2(O\text{-}t\text{-}Bu)_6(\mu\text{-}CNxylyl)$ Molecule

atom	10^4x	10^4y	10^4z	$10B_{iso}$, Å^2
W(1)	6762.9 (5)	1264.1 (4)	6610 (1)	12
W(2)	6201 (1)	625.0 (4)	7610 (1)	13
C(3)	5703 (11)	1215 (11)	6991 (13)	13 (4)
N(4)	5090 (9)	1433 (7)	6884 (10)	11 (4)
C(5)	4809 (11)	1693 (9)	6242 (12)	8 (4)
C(6)	4738 (13)	1394 (10)	5548 (14)	19 (5)
C(7)	4434 (13)	1700 (11)	4910 (14)	19 (5)
C(8)	4243 (15)	2247 (12)	4942 (17)	31 (6)
C(9)	4291 (14)	2542 (13)	5664 (15)	28 (6)
C(10)	4578 (15)	2252 (12)	6314 (16)	30 (6)
C(11)	4917 (14)	792 (11)	5479 (15)	25 (5)
C(12)	4575 (14)	2571 (12)	7053 (15)	29 (6)
O(13)	6972 (8)	2034 (7)	6568 (10)	23 (3)
C(14)	6974 (12)	2625 (10)	6831 (14)	19 (5)
C(15)	7727 (17)	2808 (13)	6920 (18)	40 (7)
C(16)	6600 (15)	2976 (12)	6237 (16)	32 (6)
C(17)	6594 (13)	2640 (11)	7600 (16)	28 (5)
O(18)	6687 (8)	1151 (7)	5521 (9)	20 (3)
C(19)	6920 (12)	1435 (10)	4795 (14)	18 (5)
C(20)	6865 (14)	979 (11)	4199 (14)	24 (5)
C(21)	6372 (13)	1883 (11)	4648 (14)	21 (5)
C(22)	7652 (14)	1645 (11)	4876 (15)	25 (5)
O(23)	7079 (8)	1143 (7)	7758 (9)	18 (3)
C(24)	7771 (13)	1093 (10)	8153 (14)	19 (5)
C(25)	8350 (14)	1160 (11)	7595 (16)	30 (5)
C(26)	7769 (14)	1592 (12)	8749 (16)	27 (6)
C(27)	7757 (13)	520 (11)	8554 (14)	23 (5)
O(28)	6955 (8)	412 (6)	6761 (9)	18 (3)
C(29)	7199 (13)	−72 (10)	6294 (14)	18 (5)
C(30)	6593 (13)	−236 (11)	5755 (15)	23 (5)
C(31)	7307 (15)	−569 (13)	6851 (16)	34 (6)
C(32)	7876 (13)	93 (11)	5864 (14)	19 (5)
O(33)	5687 (8)	−40 (7)	7343 (9)	21 (3)
C(34)	5250 (13)	−472 (10)	7673 (15)	25 (5)
C(35)	5197 (15)	−968 (12)	7063 (16)	32 (6)
C(36)	4494 (18)	−243 (14)	7802 (19)	49 (8)
C(37)	5590 (16)	−675 (13)	8463 (17)	40 (6)
O(38)	5772 (7)	756 (6)	8575 (8)	14 (3)
C(39)	5470 (12)	1144 (10)	9106 (13)	16 (5)
C(40)	4662 (15)	1047 (12)	9161 (17)	35 (6)
C(41)	5615 (14)	1741 (11)	8880 (15)	23 (5)
C(42)	5796 (13)	1007 (10)	9910 (14)	19 (5)

Table II. Selected Bond Distances (Å) for the $W_2(O\text{-}t\text{-}Bu)_6(\mu\text{-}CNxylyl)$ Molecule

A	B	dist
W(1)	W(2)	2.525 (4)
W(1)	O(13)	1.858 (16)
W(1)	O(18)	1.910 (15)
W(1)	O(23)	2.094 (15)
W(1)	O(28)	2.056 (15)
W(1)	C(3)	2.098 (21)
W(2)	O(23)	2.067 (15)
W(2)	O(28)	2.101 (15)
W(2)	O(33)	1.897 (16)
W(2)	O(38)	1.880 (14)
W(2)	C(3)	1.988 (23)
O(13)	C(14)	1.46 (3)
O(18)	C(19)	1.490 (27)
O(23)	C(24)	1.472 (27)
O(28)	C(29)	1.472 (28)
O(33)	C(34)	1.426 (28)
O(38)	C(39)	1.415 (26)
N(4)	C(3)	1.274 (27)
N(4)	C(5)	1.375 (26)

in Table I, and a view of the molecule showing the atom numbering scheme used in the tables is given in Figure 1. Selected bond distances and angles are given in Tables II and III, respectively. The local geometry about each WO_4C unit is essentially that of a square-based pyramid with the oxygen atoms occupying basal sites and the C atom of the isocyanide ligand occupying the apical position. The structural details of the $W_2(O\text{-}t\text{-}Bu)_6(\mu\text{-}CNxylyl)$ molecule

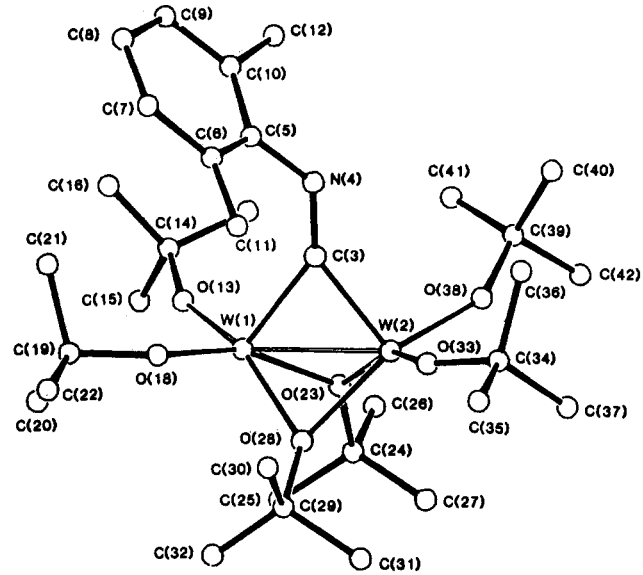

Figure 1. A ball-and-stick view of the $W_2(O\text{-}t\text{-}Bu)_6(\mu\text{-}CNxylyl)$ molecule giving the atom numbering scheme used in the tables.

Table III. Selected Bond Angles (deg) for the $W_2(O\text{-}t\text{-}Bu)_6(\mu\text{-}CNxylyl)$ Molecule

A	B	C	angle
O(13)	W(1)	O(18)	96.5 (7)
O(13)	W(1)	O(23)	96.4 (7)
O(13)	W(1)	O(28)	157.1 (6)
O(13)	W(1)	C(3)	105.5 (9)
O(18)	W(1)	O(23)	159.9 (6)
O(18)	W(1)	O(28)	90.1 (6)
O(18)	W(1)	C(3)	103.4 (8)
O(23)	W(1)	O(28)	72.3 (6)
O(23)	W(1)	C(3)	87.9 (7)
O(28)	W(1)	C(3)	94.1 (8)
O(23)	W(2)	O(28)	71.9 (6)
O(23)	W(2)	O(33)	157.4 (6)
O(23)	W(2)	O(38)	97.7 (6)
O(23)	W(2)	C(3)	91.7 (8)
O(28)	W(2)	O(33)	88.6 (6)
O(28)	W(2)	O(38)	161.6 (6)
O(28)	W(2)	C(3)	96.1 (7)
O(33)	W(2)	O(38)	97.8 (7)
O(33)	W(2)	C(3)	102.0 (8)
O(38)	W(2)	C(3)	99.4 (8)
W(1)	O(13)	C(14)	156.5 (15)
W(1)	O(18)	C(19)	138.4 (13)
W(1)	O(23)	W(2)	74.7 (5)
W(1)	O(23)	C(24)	134.6 (13)
W(2)	O(23)	C(24)	135.7 (14)
W(1)	O(28)	W(2)	74.8 (5)
W(1)	O(28)	C(29)	137.9 (14)
W(2)	O(28)	C(29)	141.1 (14)
W(2)	O(33)	C(34)	141.6 (15)
W(2)	O(38)	C(39)	148.8 (14)
C(3)	N(4)	C(5)	130.1 (19)
W(1)	C(3)	W(2)	76.3 (8)
W(1)	C(3)	N(4)	142.0 (18)
W(2)	C(3)	N(4)	141.7 (18)
N(4)	C(5)	C(6)	120.3 (19)
N(4)	C(5)	C(10)	118.0 (21)

are, not surprisingly, very similar to its $W_2(O\text{-}t\text{-}Bu)_6(\mu\text{-}CO)$ counterpart.[4] The average terminal and bridging W–O distances of 1.87 and 2.08 Å, respectively, are essentially identical between carbonyl and aryl isocyanide analogues. The W–W distance of 2.52 Å is also virtually identical while for the $W_2(\mu\text{-}CNxylyl)$ moiety the average W–C distance of 2.04 Å appears slightly longer than the carbonyl analogue by 0.04 Å. There appears to be an asymmetry in the W–C distances of 2.098 (21) and 1.988 (23) Å for W–C bonds syn and anti to the aryl group of the xylyl

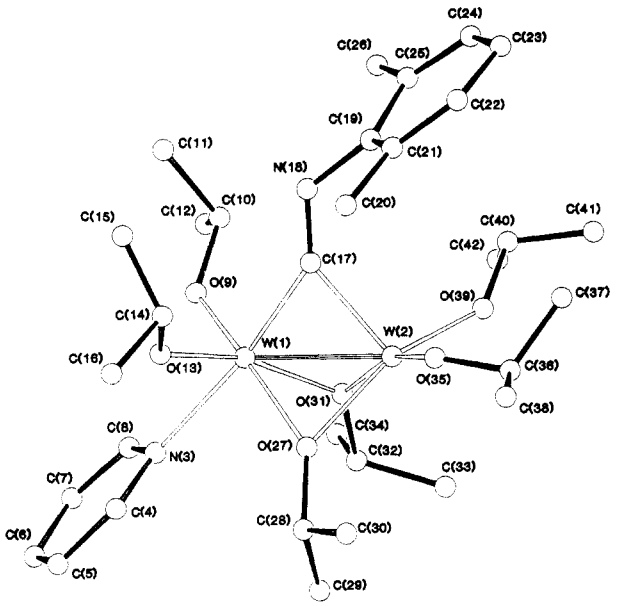

Figure 2. A ball-and-stick view of the $W_2(O\text{-}i\text{-}Pr)_6(py)(\mu\text{-}CNxylyl)$ molecule giving the atom numbering scheme used in the tables.

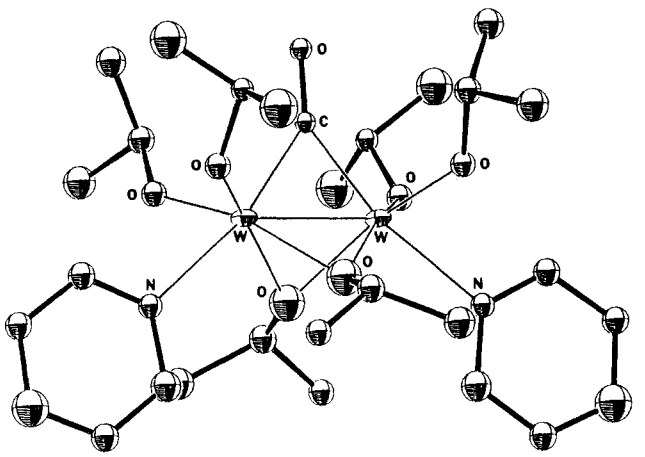

Figure 3. An ORTEP view of the $W_2(O\text{-}i\text{-}Pr)_6(py)_2(\mu\text{-}CO)$ molecule from ref 3.

isocyanide ligand, although the precision of the W–C distances is not sufficient to say more than this is an apparent trend. The bridging isocyanide ligand is bent with a C–N–C angle of 130° and aligned parallel to the M–M axis. The isocyanide C—N distance of 1.274 (27) Å is indicative of a C—N double bond and can be compared to a typical C=N distance of 1.26 Å of a benzylideneaniline, PhN=CHPh.[6]

$W_2(O\text{-}i\text{-}Pr)_6(py)(\mu\text{-}CNxylyl)$. Atomic positional parameters are given in Table IV, and a view of the molecule giving the atom number scheme used in the tables is given in Figure 2. Selected bond distances and angles are given in Tables V and VI, respectively. There are some fascinating similarities and differences between the $W_2(O\text{-}i\text{-}Pr)_6(py)_2(\mu\text{-}CO)$ and $W_2(O\text{-}i\text{-}Pr)_6(py)(\mu\text{-}CNxylyl)$ structures with respect to the observed conformations of the isoproyl groups, which can be rationalized in terms of the natural tendency to minimize steric repulsive interactions. A view of the $W_2(O\text{-}i\text{-}Pr)_6(py)_2(\mu\text{-}CO)$ molecule is shown in Figure 3 for comparison purposes. Note that the carbonyl ligand in the latter molecule fits into a pocket or cavity formed by the four methyne groups of the terminal isopropoxy ligands. It has been argued that replacement of the methyne hydrogens by methyl groups causes severe steric crowding in accordance with the inability to isolate W_2-

(6) The C=N distance for the planar *N*-(*p*-chlorobenzylidene)-*p*-chloroaniline was found to be 1.262 Å which can be compared to that found in *N*-(2,4-dichlorobenzylidene)aniline, 1.268 Å, and *N*-(*p*-methylbenzylidene)-*p*-nitroaniline, 1.269 Å. See: Bernstein, J.; Schmidt, G. M. *J. Chem. Soc., Perkin Trans. 2* **1972**, 951 and references therein.

Table IV. Fractional Coordinates and Isotropic Thermal Parameters for the $W_2(O\text{-}i\text{-}Pr)_6(py)(\mu\text{-}CNxylyl)$ Molecule

atom	10^4x	10^4y	10^4z	$10B_{iso}$, Å^2
W(1)	4969 (1)	5682 (1)	2000.1 (4)	16
W(2)	5170 (1)	5687 (1)	3281.6 (4)	20
N(3)	5484 (15)	4889 (9)	1215 (7)	15
C(4)	4612 (19)	4391 (12)	911 (11)	24
C(5)	4758 (22)	3928 (12)	407 (11)	34
C(6)	5926 (23)	4029 (12)	156 (11)	28
C(7)	6853 (21)	4552 (11)	437 (12)	23
C(8)	6576 (19)	4969 (12)	943 (11)	24
O(9)	6035 (12)	6280 (8)	1529 (6)	23
C(10)	6683 (21)	6952 (12)	1699 (11)	26
C(11)	5731 (24)	7502 (13)	1242 (12)	33
C(12)	8049 (24)	6938 (15)	1523 (12)	41
O(13)	3185 (12)	5666 (7)	1338 (7)	20
C(14)	1854 (22)	5952 (12)	1406 (10)	24
C(15)	1676 (23)	6649 (13)	1057 (12)	32
C(16)	767 (22)	5425 (13)	1015 (12)	32
C(17)	4497 (21)	6487 (14)	2586 (11)	30
N(18)	4132 (18)	7110 (9)	2561 (8)	30
C(19)	3949 (23)	7515 (13)	3119 (10)	27
C(20)	1572 (22)	6891 (14)	3007 (12)	32
C(21)	2681 (21)	7408 (11)	3360 (11)	23
C(22)	2542 (22)	7802 (13)	3927 (11)	30
C(23)	3528 (25)	8293 (14)	4262 (11)	37
C(24)	4680 (21)	8417 (13)	3954 (13)	32
C(25)	4860 (19)	8067 (12)	3397 (11)	22
C(26)	6030 (25)	8216 (12)	3086 (11)	40
O(27)	4358 (16)	4890 (8)	2577 (7)	25
C(28)	3835 (23)	4172 (10)	2577 (11)	25
C(29)	4955 (42)	3686 (14)	2679 (24)	124
C(30)	2839 (38)	4105 (21)	2994 (23)	109
O(31)	6705 (12)	5415 (7)	2788 (6)	20
C(32)	7742 (21)	4875 (12)	2880 (10)	24
C(33)	8125 (24)	4658 (14)	3640 (13)	39
C(34)	9014 (26)	5143 (15)	2655 (13)	42
O(35)	2645 (14)	5624 (9)	3716 (7)	30
C(36)	3499 (22)	5504 (11)	4378 (11)	25
C(37)	3787 (42)	6137 (19)	4810 (20)	108
C(38)	2151 (41)	5237 (22)	4396 (17)	106
O(39)	6422 (15)	6131 (8)	4017 (7)	25
C(40)	7280 (28)	6735 (13)	4192 (13)	42
C(41)	7478 (40)	6822 (24)	4933 (21)	142
C(42)	8633 (41)	6624 (23)	4051 (23)	123

Table V. Selected Bond Distances (Å) for the $W_2(O\text{-}i\text{-}Pr)_6(py)(\mu\text{-}CNxylyl)$ Molecule

A	B	dist
W(1)	W(2)	2.500 (2)
W(1)	O(9)	1.941 (14)
W(1)	O(13)	1.928 (12)
W(1)	O(27)	2.074 (13)
W(1)	O(31)	2.087 (12)
W(1)	N(3)	2.317 (15)
W(1)	C(17)	2.048 (28)
W(2)	O(27)	2.092 (14)
W(2)	O(31)	2.063 (12)
W(2)	O(35)	1.913 (13)
W(2)	O(39)	1.875 (13)
W(2)	C(17)	2.060 (22)
O(9)	C(10)	1.436 (25)
O(13)	C(14)	1.460 (23)
O(27)	C(28)	1.462 (23)
O(31)	C(32)	1.433 (26)
O(35)	C(36)	1.380 (24)
O(39)	C(40)	1.42 (3)
N(3)	C(4)	1.327 (25)
N(3)	C(8)	1.329 (25)
N(18)	C(17)	1.24 (3)
N(18)	C(19)	1.398 (27)

Table VI. Selected Bond Angles (deg) for the $W_2(O\text{-}i\text{-}Pr)_6(py)(\mu\text{-}CNxylyl)$ Molecule

A	B	C	angle
O(9)	W(1)	O(13)	101.1 (5)
O(9)	W(1)	O(27)	163.8 (6)
O(9)	W(1)	O(31)	93.6 (5)
O(9)	W(1)	N(3)	79.9 (6)
O(9)	W(1)	C(17)	93.4 (7)
O(13)	W(1)	O(27)	91.5 (6)
O(13)	W(1)	O(31)	163.3 (6)
O(13)	W(1)	N(3)	81.0 (5)
O(13)	W(1)	C(17)	96.0 (7)
O(27)	W(1)	O(31)	72.7 (6)
O(27)	W(1)	N(3)	92.2 (6)
O(27)	W(1)	C(17)	95.4 (7)
O(31)	W(1)	N(3)	94.1 (5)
O(31)	W(1)	C(17)	90.9 (6)
N(3)	W(1)	C(17)	171.9 (7)
O(27)	W(2)	O(31)	72.8 (5)
O(27)	W(2)	O(35)	92.4 (6)
O(27)	W(2)	O(39)	157.7 (6)
O(27)	W(2)	C(17)	94.5 (7)
O(31)	W(2)	O(35)	161.7 (7)
O(31)	W(2)	O(39)	93.6 (6)
O(31)	W(2)	C(17)	91.2 (8)
O(35)	W(2)	O(39)	96.8 (6)
O(35)	W(2)	C(17)	100.9 (8)
O(39)	W(2)	C(17)	103.5 (8)
W(1)	O(9)	C(10)	132.4 (12)
W(1)	O(13)	C(14)	128.7 (11)
W(1)	O(27)	W(2)	74.1 (5)
W(1)	O(27)	C(28)	146.3 (12)
W(2)	O(27)	C(28)	139.2 (12)
W(1)	O(31)	W(2)	74.4 (4)
W(1)	O(31)	C(32)	134.8 (11)
W(2)	O(31)	C(32)	134.9 (12)
W(2)	O(35)	C(36)	135.9 (13)
W(2)	O(39)	C(40)	143.0 (14)
W(1)	N(3)	C(4)	123.4 (12)
W(1)	N(3)	C(8)	122.3 (14)
C(4)	N(3)	C(8)	113.4 (16)
C(17)	N(18)	C(19)	126.1 (22)
N(3)	C(4)	C(5)	128.6 (17)
W(1)	C(17)	W(2)	75.3 (9)
W(1)	C(17)	N(18)	143.2 (17)
W(2)	C(17)	N(18)	141.3 (19)
N(18)	C(19)	C(21)	118.1 (21)
N(18)	C(19)	C(25)	122.1 (19)

$(O\text{-}t\text{-}Bu)_6(py)_2(\mu\text{-}CO)$ compounds.[3] It can be seen in Figure 2 that the isopropoxide ligands syn to the xylyl group of the isocyanide ligand bend away from the xylyl group to minimize steric pressure. Presumably, the resultant crowding at the W atom syn to the xylyl moiety disfavors pyridine coordination to this site. The W–W distance of 2.510 (2) Å is virtually identical, within experimental limits, with that found for $W_2(O\text{-}i\text{-}Pr)_6(py)_2(\mu\text{-}CO)$.[3] The W–C and C–N bonds in the $W_2(\mu\text{-}CNxylyl)$ unit are 2.05 (averaged) and 1.24 Å, respectively, and the CNxylyl moiety is bent parallel to the M–M axis with a C–N–C angle of 126°. The W–N distance of 2.32 Å is relatively long for coordinated py compared to the W–N distance of 2.08 Å in $W_2(O\text{-}i\text{-}Pr)_6(py)_2$.[7] There are two distinct terminal W–O distances for the tungsten atoms with and without coordinated pyridine. For the tungsten atom with coordinated pyridine, the terminal W–O distances average 1.93 Å with W–O–C angles of 130°. By comparison, the tungsten atom without coordinated pyridine displays a shorter terminal W–O distance of 1.89 Å (averaged) with W–O–C angles on the order of 140°. In general, the shorter W–O distance and more obtuse W–O–C angle correspond to greater oxygen-to-metal π-donation.[8]

(7) Akiyama, M.; Chisholm, M. H.; Cotton, F. A.; Extine, M. W.; Haitko, D. A.; Little, D.; Fanwick, P. E. *Inorg. Chem.* **1979**, *18*, 2266.

Infrared and NMR Spectroscopic Studies. Infrared spectra of metal isocyanide complexes may provide a convenient source of information concerning the structure and bonding of the isocyanide ligand bound to a transition metal. For neutral molecules with bridging isocyanide ligands, the μ-CNR moiety displays a C–N stretching frequency in the range from 1700 to 1870 cm^{-1}.[9] The new $W_2(\mu\text{-}CNR)$ containing compounds display low ν(C–N) values near 1530 cm^{-1} which are unusually low when compared to those of known organometallic complexes with the μ-CNR ligand.[9] The values of ν(C–N) are remarkably low for a bridging isocyanide ligand and are actually on the order of 100 cm^{-1} lower than the typical C=N stretching frequency of purely aliphatic imines, $R_2C{=}NR$, which display ν(C=N) near 1670 cm^{-1}, or a typical Schiff's base which displays ν(C=N) near 1640 cm^{-1}.[10] In fact, the C–N stretch is more similar to that of an amino carbyne ligand (μ-CNRH), like that recently reported by Kubiak and co-workers which displays ν(C=N) near 1525 cm^{-1}.[11]

The ^{13}C NMR spectra can be very useful, and the bridging carbon atom is generally found between 220 and 260 ppm downfield from Me_4Si, which is at much lower field than terminal isocyanide groups.[9b] The ^{13}C NMR spectra of isocyanide ligands are often difficult to obtain due to the long relaxation times (T_1) of the isocyanide carbon.[9] We have obtained natural abundance $^{13}C\{^1H\}$ spectra of these compounds by employing $Cr(acac)_3$ as a shiftless relaxation reagent[12] and long preaquisition delay times of up to 8 s. Our primary interest was to obtain both the ^{13}C chemical shift and the ^{183}W–^{13}C coupling constant for comparison with the $W_2(\mu\text{-}CO)$ containing compounds. Only for the case of $W_2(O\text{-}t\text{-}Bu)_6(\mu\text{-}CN\text{-}t\text{-}Bu)$ was the solubility in toluene-d_8 sufficient to allow for accurate determination of ^{183}W–^{13}C coupling information. The isocyanide carbon is found at 281 ppm with ^{183}W–^{13}C coupling of 140 Hz. This is only slightly upfield from the $W_2(O\text{-}t\text{-}Bu)_6(\mu\text{-}CO)$ analogue where the carbonyl carbon is found at 291 ppm with ^{183}W–^{13}C coupling of 193 Hz.[4] These low values of ν(C=N) and $\delta(^{13}C)$ are consistent with a high degree of π back-bonding from W d orbitals to the vacant high-energy π^* orbitals of the isocyanide ligand and show a remarkable parallel to the bridging carbonyl analogues where we have attributed the low values of ν and

(8) For listings and discussion of M–M and M–O distances in the chemistry of molybdenum and tungsten alkoxides see: (a) Chisholm, M. H. *Polyhedron* **1983**, *2*, 681. For a theoretical discussion of M–O distance and M–O–C angle variations and their effect on oxygen-to-metal π-donation see: (b) Chisholm, M. H.; Clark, D. L. *Comments Inorg. Chem.* **1987**, *6*, 23.

(9) Excellent reviews on transition-metal isocyanide complexes exist, see: (a) Singleton, E.; Oosthuizen, H. E. *Adv. Organomet. Chem.* **1983**, *22*, 209 and references therein. (b) Yamamoto, Y. *Coord. Chem. Rev.* **1980**, *32*, 193 and references therein. (c) Treichel, P. M. *Adv. Organomet. Chem.* **1973**, *11*, 21. An excellent discussion on infrared and ^{13}C NMR spectroscopy of transition-metal isocyanide complexes can be found in ref 9b.

(10) For a general discussion of the C=N stretching frequency see: (a) Patai, S. *The Chemistry of the Carbon-nitrogen Double Bond*; Interscience: *New* York, 1970; p 37. A detailed analysis of the factors influencing the C=N stretching frequency in Schiff's bases has recently appeared, see: (b) Lopez-Garriga, J. J.; Babcock, G. T.; Harrison, J. F. *J. Am. Chem. Soc.* **1986**, *108*, 7241.

(11) (a) Delaet, D. L.; Fanwick, P. E.; Kubiak, C. P. *Organometallics* **1986**, *5*, 1807. Other amino carbynes have been prepared from isocyanides, see: (b) Basset, J. M.; Barker, G. K.; Green, M.; Howard, J. A. K.; Stone, F. G. A.; Wolsey, W. C. *J. Chem. Soc., Dalton Trans.* **1981**, 219. (c) Pombeiro, A. J. L.; Richards, R. L. *Transition Met. Chem. (Weinheim, Ger.)* **1980**, *5*, 281. (d) Churchhill, M. R.; DeBoer, B. G.; Rotella, F. J. *Inorg. Chem.* **1976**, *15*, 1843. (e) Adams, R. D.; Golembeski, N. M. *Inorg. Chem.* **1979**, *18*, 2255. (f) Willis, S.; Manning, A. R. *J. Chem. Soc., Dalton Trans.* **1981**, 322.

(12) Gansow, O. A.; Burke, A. R.; LaMar, G. N. *J. Chem. Soc., Chem. Commun.* **1972**, 456.

δ to the oxycarbyne character of the $M_2(\mu\text{-CO})$ unit.[4] In both of these regards, the new isocyanide compounds reported here show anomalous spectroscopic properties.

Dynamical Solution Behavior. At room temperature in toluene-d_8 and benzene-d_6 solution, ^{1}H NMR spectra indicate rapid exchange of terminal and bridging alkoxide ligands. Furthermore, in the case of the xylyl isocyanide there is evidently an equilibrium between two isomeric forms of the molecule in solution. This may involve an equilibrium between μ-CNR and μ-η^2-CNR ligands, and further studies of this phenomenon are in progress.[13] Upon a lowering of the temperature, the minor isomer disappears, the initially sharp resonances broaden and then collapse, and finally, below −80 °C at 360 MHz, we obtain a low-temperature-limiting spectrum that is reconcilable with the structure found in the solid state. Specifically, the low-temperature ^{1}H NMR spectra show two types of OR ligands in the ratio 2:1, and the methyl protons of the O-*i*-Pr groups are diastereotopic. The observation of a 2:1 ratio of terminal to bridging OR ligand indicates that there is still a fluxional process occurring at the isocyanide ligand which makes the two ends of the M_2 unit equivalent. Presumably this proceeds via nitrogen inversion involving a linear transition state, and this process cannot be frozen out even at −95 °C.[14] This fluxional process is depicted in I.

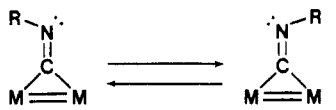

I

Electronic Structure and Bonding in $W_2(\mu$-CNR)-Containing Compounds. The solid-state molecular structure of $W_2(O\text{-}t\text{-}Bu)_6(\mu\text{-CNxylyl})$ poses several fascinating questions about the bonding in the $W_2(\mu$-CNR) moiety. Specifically, we were interested in the origin of the apparent asymmetry in the W–C bond distances and the bending of the C–N–R moiety parallel to the M–M axis. Furthermore, the spectroscopic data are consistent with substantial carbyne character in the W–C bonds by analogy to the $W_2(\mu$-CO)-containing compounds. Finally, our previous theoretical studies on the $M_2(OR)_6(\mu$-CO) unit[5] provided valuable insight into the synthetic strategy that led to the successful isolation of $W_2(OR)_6(\mu$-CNR) compounds. Now that the isolation of these compounds has reached fruition, we are in the unique position to continue our theoretical studies by comparing the bonding of bridging carbonyl and isocyanide ligands in *identical molecular environments*. We achieve this by employing model compounds of formula $W_2(OH)_6(\mu$-CNR) where R = H or CH_3. This model will facilitate a direct comparison to our previous results on the analogous carbonyl system.

Free Ligand Results. After each calculation is completed in an atomic basis set, it is useful to transform the results into a basis set consisting of the molecular orbitals of the isolated isocyanide or carbonyl ligand and dimetal fragments. The utility of this procedure is that it effectively isolates in a few of the free ligand and dimetal fragment orbitals those population changes which result from direct metal–ligand bonding interactions. The molecular orbitals for the free C≡X ligands (X = O, NH, NCH_3) were calculated at the C–X distances found in the $W_2(\mu$-CX)-containing compounds. The CO and CNH ligands have $C_{\infty v}$ symmetry, and the 1π and 2π (π and π^*, respectively) orbital pairs are degenerate, and the 5σ carbon lone-pair orbital is the HOMO. For the methyl isocyanide ligand, the 2e, $7a_1$, and 3e orbitals correspond to the 1π, 5σ, and 2π orbitals of CNH and CO, respectively. For simplicity, we will retain the 5σ and 1π nomenclature for all C≡X ligands throughout this work. The overlap populations for the important 1π, 5σ, and 2π valence orbitals of the free C≡X ligands (X = O, NH, NCH_3) are listed in Table VII. The slightly negative overlap population of the 5σ carbon lone-pair orbital indicates the slight antibonding character in the C≡X region compared to the strongly antibonding 2π orbital. A molecular orbital diagram comparing the valence 5σ and 2π orbitals of methyl isocyanide to linear and bent hydrogen isocyanide at the C–N distances in $W_2(\mu$-CNR) compounds is shown in

Table VII. Overlap Populations[a] for an Uncoordinated C≡X Ligand at the Internuclear Distances Relevant for Free C≡X and the C≡X Moiety in $W_2(\mu$-CX)-Containing Compounds, Where X = O, NH, or NCH_3

ligand	R, Å	$1\pi_\perp$	$1\pi_\parallel$	5σ	$2\pi_\perp$	$2\pi_\parallel$
C≡O	1.130	0.237	0.237	−0.175	−0.508	−0.508
C≡O	1.250	0.206	0.206	−0.139	−0.395	−0.395
C≡NH	1.160	0.275	0.275	−0.048	−0.683	−0.683
C≡NH	1.247	0.252	0.252	−0.043	−0.576	−0.576
C≡NH(bent)	1.247	0.254	0.216	−0.056	−0.577	−0.446
C≡NCH_3	1.166	0.271	0.271	−0.045	−0.680	−0.680
C≡NCH_3	1.247	0.247	0.247	−0.040	0.584	−0.584
C≡NCH_3(bent)	1.247	0.255	0.216	−0.043	−0.583	−0.483

[a] Overlap population between C and X for a single electron occupying the molecular orbital.

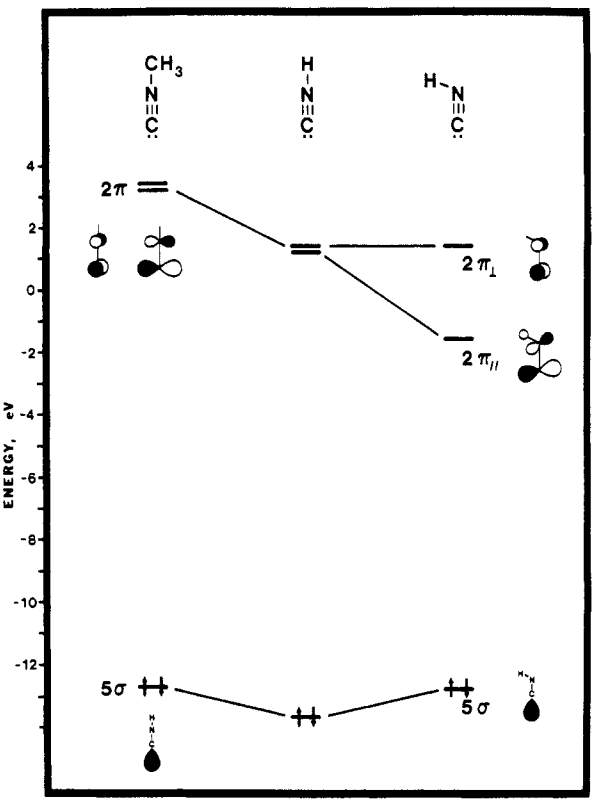

Figure 4. Molecular orbital diagram comparing the valence orbitals of methyl isocyanide to linear and bent (CNH = 130°) hydrogen isocyanide at the C—N distances in $W_2(\mu$-CNR) compounds.

(13) For studies on the μ-η^2-CNR ligand see: (a) Brunner, H.; Buchner, H.; Wachter, J.; Bernal, I.; Reis, W. H. *J. Organomet. Chem.* **1983**, *244*, 247. (b) Adams, R. D.; Katahira, D. A.; Yang, L.-W. *Organometallics* **1982**, *1*, 231. (c) Benner, L. S.; Olmstead, M. M.; Balch, A. L. *J. Organomet. Chem.* **1978**,*159*, 289. (d) Balch, A. L.; Benner, L. S. *J. Organomet. Chem.* **1977**, *135*, 339.

(14) Nitrogen inversion of bridging isocyanide ligands is well-established, see: (a) Adams, R. D.; Cotton, F. A. *Inorg. Chem.* **1974**, *13*, 249. (b) Cotton, F. A.; Frenz, B. A. *Inorg. Chem.* **1974**, *13*, 253. (c) Adams, R. D.; Cotton, F. A.; Troup, J. M. *Inorg. Chem.* **1974**, *13*, 257. (d) Howell, J. A. S.; Rowan, A. J. *J. Chem. Soc., Dalton Trans.* **1980**, 503.

Figure 4. The greater electron-withdrawing nature of H relative to CH_3 results in a lowering of both the 5σ and 2π orbitals of HNC relative to CH_3NC. Since the 5σ and 2π orbital energetics will be important in terms of metal–ligand bonding in $W_2(\mu\text{-CNR})$ compounds, we feel that the CH_3NC ligand is a more appropriate model for comparison with our earlier results on $W_2(\mu\text{-CO})$-containing compounds. Bending the isocyanide ligand in the plane of the page lowers the symmetry and lifts the degeneracy of the 1π and 2π orbitals. Retaining the $1\pi/2\pi$ nomenclature, we define $\pi_\perp$ and $\pi_\parallel$ orbitals of the bent C–N–H ligand as those π orbitals perpendicular or parallel to the C–N–H bending plane (respectively) as shown in Figure 4. The energy of the $2\pi_\perp$ orbital is essentially independent of C–N–H angle because on bending, the hydrogen atom moves on the nodal plane and therefore the H 1s orbital cannot contribute to the $2\pi_\perp$ orbital. In the $2\pi_\parallel$ orbital, bending moves the hydrogen off the nodal plane and allows for in-phase H 1s mixing with the N $p\pi_\parallel$ orbital. This results in a stabilization and a decrease in the C–N antibonding character of the orbital as revealed in the C–N overlap populations of Table VII. A secondary effect of bending is a mixing of the $1\pi_\parallel$ and 5σ orbitals which have the same symmetry on bending and result in a slight stabilization of the $1\pi_\parallel$ (not shown in Figure 4) and destabilization of the 5σ orbitals.[15] These energy changes that occur in the isocyanide ligand upon bending will have important consequences toward the bonding interactions between the isocyanide ligand and the $W_2(OH)_6$ fragment.

The C_{2v} $W_2(OH)_6$ Fragment. Perhaps one of the easiest ways to visualize the bonding interactions between the CX ligand and the W_2 unit in the $W_2(\mu\text{-CX})$-containing compounds is to examine the interactions in terms of fragment MO's. Our initial model compound of formula $W_2(OH)_6(\mu\text{-CNR})$ can be conveniently decomposed into $W_2(OH)_6$, having C_{2v} symmetry, and CNR fragments (R = H, CH_3). The important metal-based fragments of C_{2v} $W_2(OH)_6$ are shown schematically in II along with a local

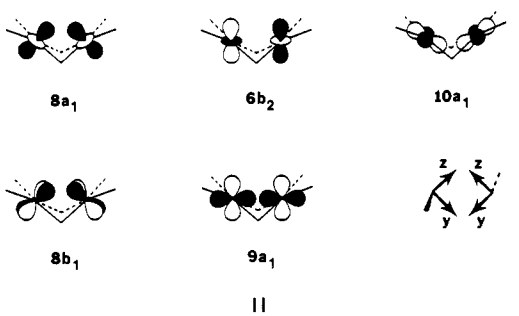

II

coordinate system on each W atom. With use of this local coordinate system, the important metal-localized fragment MO's of C_{2v} $W_2(OH)_6$ can be easily visualized in terms of combining two square-planar metal fragments "hinged" along a common edge. In- and out-of-phase combinations of two metal d_{z^2} atomic orbitals yield the $8a_1$ and $6b_2$ M–M σ-bonding and -antibonding fragment MO's, respectively. In a similar fashion, the in-phase combinations of two d_{xz} and d_{yz} atomic orbitals would give rise to the $8b_1$ and $9a_1$ M–M π- and σ-bonding fragment MO's, respectively. The last fragment orbital important to our analysis can be

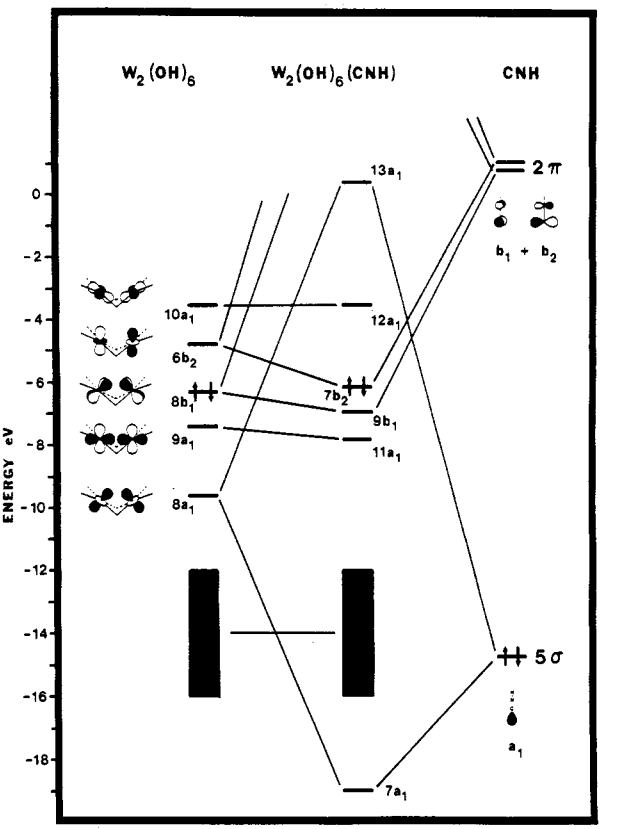

Figure 5. Fragment molecular orbital diagram showing the perturbation of C_{2v} $W_2(OH)_6$ fragment orbitals by interaction with a linear CNH moiety. The HOMO in each case is denoted by arrows. Only the important metal- and isocyanide-localized fragments are shown.

thought of as an in-phase combination of two $d_{x^2-y^2}$ atomic orbitals which gives rise to the $10a_1$ M–M σ-bonding fragment MO of C_{2v} $W_2(OH)_6$. The six metal d electrons occupy the $8a_1$, $9a_1$, and $8b_1$ M–M bonding orbitals as seen on the left of Figure 5. The M–M σ-bonding $10a_1$ fragment orbital is unoccupied and lies very high in energy as a result of strong π-donor interactions with the OH^- ligands, and this phenomenon has been discussed in detail elsewhere.[5]

$W_2(OH)_6(\mu\text{-CNR})$ and the Nature of M–C and M–M Bonding (R = H, CH_3). We will first examine the bonding in a model compound of formula $W_2(OH)_6(\mu\text{-CNR})$ with a linear C–N–R moiety and R = H or CH_3 employing the Fenske–Hall method.[16] This approach is meant to illustrate the striking bonding similarities between the isocyanide calculations presented here (X = NH, NCH_3) and our previous calculations on the carbonyl analogues (X = O).[5] Beginning with a linear C–N–R moiety, we facilitate a direct comparison of those population changes that occur in the C–N–R ligand as a result of M–C bonding interaction and subsequent C–N–R angle bending.

As in our previous studies on $W_2(\mu\text{-CO})$-containing compounds, we find that only the 5σ and 2π orbitals of linear CNR (R = H, CH_3) have any appreciable interaction with the C_{2v} $W_2(OH)_6$ fragment. The bonding between the W_2 center and the isocyanide ligand can be adequately described by a σ-bonding and π back-bonding process whereby the isocyanide 5σ carbon lone-pair orbital donates electron density to the W_2 unit and the W_2 center back-donates electron density from filled metal d-orbitals to the unoccupied 2π (or π^*) orbitals of the isocyanide ligand. This is summarized for R = H in the correlation diagram

(15) Ab initio calculations on free HNC reveal that it is easily bent, see: (a) Nguyen, M. T.; Hegarty, A. F.; Sana, M.; Leroy, G. *J. Am. Chem. Soc.* **1985**, *107*, 4141. Ab initio calculations on CH_3NC in linear and bent geometries arrive at similar conclusions to those presented here with respect to the σ-donor and π-acceptor properties, yet differ with respect to the ordering of occupied MO's of the free ligand in the bent geometry, see: (b) Howell, J. A. S.; Saillard, J.-Y.; Le Beuze, A.; Jeouen, G. *J. Chem. Soc., Dalton Trans.* **1982**, 2533.

(16) Hall, M. B.; Fenske, R. F. *Inorg. Chem.* **1972**, *11*, 768.

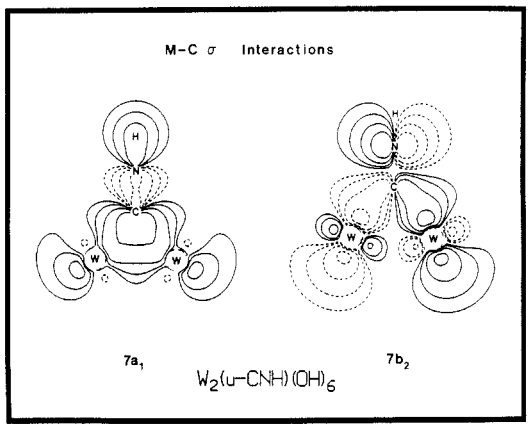

Figure 6. Contour plots of the $7a_1$ and $7b_2$ W–C σ-bonding orbitals of $W_2(OH)_6(\mu$-CNH) with the linear CNH moiety. Plots represent a slice taken through the plane containing the $W_2(\mu$-CNH) moiety. Dashed lines represent negative wave function values, and solid lines represent positive values. Contour values are ±0.02, ±0.04, ±0.08, and ±0.16 e/Å^3 in this and all subsequent plots.

shown in Figure 5. As shown in Figure 5, the linear CNH 5σ carbon lone-pair orbital has a_1 symmetry in the C_{2v} point group and can interact with W_2 fragment MO's of the same symmetry. From simple perturbation theory, the magnitude of the interaction will depend on the relative orbital energetics and magnitude of overlap between CNH and $W_2(OH)_6$ fragment orbitals. The primary interaction is with the $8a_1$ M–M σ-bonding orbital of $W_2(OH)_6$ since it is energetically more accessible and has the best overlap with the CNH 5σ orbital. This interaction results in the formation of the $7a_1$ and $13a_1$ M–C σ-bonding and -antibonding MO's of $W_2(OH)_6(\mu$-CNH), respectively. The $7a_1$ orbital is predominantly CNH 5σ in character, and the $13a_1$ orbital is predominantly metal d_{z^2} in character with some valence metal s and p_z mixing as a result of the W–C interaction. The $9a_1$ and $10a_1$ $W_2(OH)_6$ fragment orbitals also have the correct symmetry to interact with the CNH 5σ orbital, but they have negligible overlap, and, as a result, these fragment MO's are virtually unperturbed by the CNH ligand and become the $11a_1$ and $12a_1$ MO's of $W_2(OH)_6(\mu$-CNH).

The CNH 2π orbitals have b_1 and b_2 symmetry in the C_{2v} point group, and we shall refer to these as $2\pi_\perp$ (b_1) and $2\pi_\parallel$ (b_2) since they can interact with $W_2(OH)_6$ fragment orbitals that are either perpendicular (b_1) or parallel (b_2) with respect to the M–M axis. The $2\pi_\parallel$ (b_2) MO of CNH has a strong, covalent interaction with the $6b_2$ $W_2(OH)_6$ fragment MO resulting in the $7b_2$ M–C σ-bonding orbital of $W_2(OH)_6(\mu$-CNH). The $2\pi_\perp$ (b_1) MO of CNH interacts predominantly with the $8b_1$ $W_2(OH)_6$ fragment orbital resulting in the formation of the $9b_1$ M–C π-bonding orbital of $W_2(OH)_6(\mu$-CNH). Methyl isocyanide gives a similar result, and thus for $W_2(OH)_6(\mu$-CNR) compounds (R = H, CH_3) we have the components of two M–C σ- and one M–C π-bonding orbitals, and the net M–C interaction is best described as "carbyne-like" in character consistent with the ^{13}C NMR chemical shift values. These three M–C bonding orbitals are shown qualitatively in III. Contour

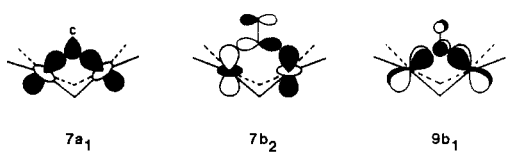

III

plots of the $7a_1$ and $7b_2$ M–C σ-bonding orbitals of $W_2(OH)_6(\mu$-CNH) are shown in Figure 6. These plots are taken as a slice through the plane containing the $W_2(\mu$-CNH) moiety and can be compared to the qualitative drawings shown in III. The plots illustrate that the $7a_1$ orbital is primarily CNH 5σ in character while the $7b_2$ orbital represents a strong, covalent back-bonding interaction between $W_2(OH)_6$ and CNH $2\pi_\parallel$ orbitals.

Table VIII. Overlap Populations between $W_2(OH)_6$ and C≡X Fragment Orbitals in $W_2(OH)_6(\mu$-CX) Compounds, Where X = O, NH, or NCH_3

ligand	$2\pi\|8b_1$	$2\pi\|6b_2$	$5\sigma\|8a_1$
C≡O	0.307	0.396	0.456
C≡NH(linear)	0.267	0.355	0.481
C≡NH(bent)	0.253	0.367	0.453
C≡NCH_3(linear)	0.247	0.332	0.461
C≡NCH_3(bent)	0.234	0.359	0.425

The W–W distances of ca. 2.5 Å in the $W_2(\mu$-CNR)-containing compounds reported here are in the range expected for a W–W double bond.[17] The presence of bridging ligands makes a formal bond order definition somewhat ambiguous since the $7a_1$ and $9b_1$ W–C bonding orbitals are also W–W bonding in character. Occupation of these orbitals will therefore contribute to *both* W–C and W–W bonding. The Mulliken populations of the $8a_1$ and $8b_1$ orbitals of $W_2(OH)_6$ in the $W_2(OH)_6(\mu$-CNH) compound are 1.0 and 1.6 electrons, respectively, and reveal the residual M–M bonding electron density in the W–C bonding orbitals of $W_2(OH)_6(\mu$-CNR) compounds.

Comparison of the Bonding Behavior of Isocyanide and Carbonyl in $W_2(\mu$-CX)-Containing Compounds and the Pronounced Effect of Isocyanide Bending. We are now in the unique position to examine the similarities and differences of the bridging isocyanide and carbonyl ligands in *identical molecular environments*. The overall $W_2(\mu$-CX) bonding picture is found to be virtually identical for both carbonyl and isocyanide ligands with the primary difference being in the CX fragment orbital energetics and magnitude of overlap with $W_2(OH)_6$ fragment orbitals. The traditional view of carbonyl vs. isocyanide bonding to a transition metal has been that isocyanide is a stronger σ donor and weaker π acceptor than carbonyl.[18] The eigenvalues of the free C≡O and C≡NCH_3 ligands and photoelectron spectroscopic data support this view.[19] The higher the 5σ HOMO energy, the better the σ-donating ability, and the lower the 2π LUMO energy, the better the 2π accepting ability. However, the C–X bond in the $W_2(\mu$-CX)-containing compounds is elongated relative to the free ligand, and this has a profound effect on both the overlap population (Table VII) and energetics of the valence orbitals. A molecular orbital diagram comparing the valence 5σ and 2π orbitals of CO to linear and bent CNH at the C–X distances in $W_2(\mu$-CX) compounds is shown in Figure 7. The orbital energies shown in Figure 7 are *not* the eigenvalues for the free C≡X ligand but,

(17) The short W–W distance of 2.5 Å is clearly indicative of some degree of multiple bonding and can be compared to the W–W double bond distances of 2.45 Å in $W_4H_2(O\text{-}i\text{-}Pr)_{14}$: (a) Akiyama, M.; Little, D.; Chisholm, M. H.; Haitko, D. A.; Cotton, F. A.; Extine, M. W. *J. Am. Chem. Soc.* **1979**, *101*, 2504. The 2.48 Å distance in $W_2Cl_4(OMe)_4(MeOH)_2$: (b) Anderson, L. B.; Cotton, F. A.; DeMarco, D.; Fang, A.; Ilsley, W. H.; Kolthammer, B. W. S.; Walton, R. A. *J. Am. Chem. Soc.* **1981**, *103*, 5078.

(18) Cotton, F. A.; Wilkinson, G. *Advanced Inorganic Chemistry*, 4th ed.; Wiley: New York, 1980.

(19) The valence photoelectron spectrum of CO may be found in many general texts and (a) Al-Joboury, M. I.; et al. *J. Chem. Soc.* **1965**, 616. The valence photoelectron spectra of several free isocyanide ligands have been reported, see: (b) Turner, D. W.; Baker, C.; Baker, A. D.; Brundle, C. R. *Molecular Photoelectron Spectroscopy*; Wiley-Interscience: London, 1977. (c) Young, V. Y.; Cheng, K. L. *J. Electron Spectrosc. Relat. Phenom.* **1976**, *9*, 317.

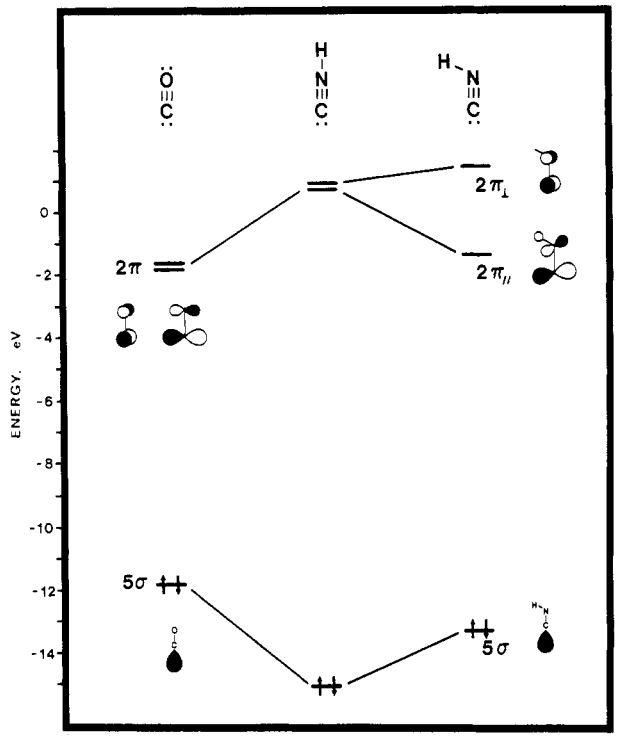

Figure 7. Molecular orbital diagram comparing the diagonal Fock matrix elements of the valence orbitals of CO to linear and bent CNH in converged calculations of $W_2(OH)_6(\mu\text{-CX})$ compounds (X = O, NH).

rather, are the diagonal Fock matrix elements for the CX moiety in converged calculations of $W_2(OH)_6(\mu\text{-CX})$ compounds (X = O, NH). This provides a convenient method for comparing the *relative* energetics of the C≡X ligand orbitals in terms of interaction with the C_{2v} $W_2(OH)_6$ fragment. From Figure 7, the 2π orbitals of the carbonyl are lower in energy than the 2π orbitals of the linear isocyanide. Thus for back-bonding, the CO 2π orbitals are energetically closer and have better overlap with $W_2(OH)_6$ fragment orbitals than their isocyanide counterparts. This latter effect is revealed in the overlap populations between valence CX ligand and $W_2(OH)_6$ fragment orbitals shown in Table VIII where it is clear that the CO 2π orbitals have greater overlap with $W_2(OH)_6$ than linear or bent CNR (R = H, CH_3) ligands. By contrast, the overlap populations (Table VIII) and orbital energetics (Figure 7) of the CX 5σ orbitals reveal opposing effects.

We can gain a more quantitative measure of the *relative* σ-donor and π-acceptor ability of these ligands by examination of the Mulliken populations[20] (or orbital occupancies) of the canonical orbitals of the CX moiety in the $W_2(\mu\text{-CX})$ compounds listed in Table IX. Since the 2π orbitals are virtual in the free ligands, an occupation greater than zero represents the amount of back-bonding from metal d orbitals to the CX ligand. In a similar fashion, an occupation less than 2.00 for the 5σ orbital represents the amount of σ-donation from the 5σ orbital to metal d orbitals. From Table IX, the synergistic nature of the $W_2(\mu\text{-CX})$ bonding is demonstrated via the loss of 5σ density and the gain of 2π density for all CX ligands (X = O, NH, NCH_3). These population changes occur as a result of direct metal–ligand bonding and reveal a measure of the *relative* magnitude of 5σ donation and 2π acceptance by carbonyl *relative* to isocyanide in the *identical molecular environment*. It can be seen from Table IX that CO is a better π-acceptor than linear CNR

(20) Mulliken, R. S. *J. Chem. Phys.* **1955**, *23*, 1833.

Table IX. Selected Mulliken Populations of the Canonical Orbitals of Free CX and the CX Moiety in $W_2(\mu\text{-CX})$-Containing Compounds, Where L = NH_3 and X = O, NH, or NCH_3

compd	5σ	$2\pi_\parallel$ [a]	$2\pi_\perp$ [b]
CO	2.000	0.000	0.000
CNH	2.000	0.000	0.000
$W_2(OH)_6(\mu\text{-CO})$	1.343	0.835	0.530
$W_2(OH)_6(\mu\text{-CNH})$(linear)	1.324	0.683	0.421
$W_2(OH)_6(\mu\text{-CNH})$(bent)	1.323	0.847	0.381
$W_2(OH)_6(\mu\text{-CNCH}_3)$(linear)	1.370	0.617	0.382
$W_2(OH)_6(\mu\text{-CNCH}_3)$(bent)	1.376	0.796	0.347
$W_2(OH)_6L_2(\mu\text{-CO})$	1.412	0.975	0.492
$W_2(OH)_6L_2(\mu\text{-CNH})$(linear)	1.397	0.798	0.398
$W_2(OH)_6L_2(\mu\text{-CNH})$(bent)	1.390	1.006	0.345

[a] $2\pi_\parallel$ is the π^* orbital parallel to the W–W axis. [b] $2\pi_\perp$ is the π^* orbital perpendicular to the W–W axis.

(R = H, CH_3) as evidenced by the larger 2π orbital occupation of CO than CNR ligands. However, the CO and CNR 5σ populations are very nearly the same, and it is concluded that the σ-donor strength of carbonyl and isocyanide in the $W_2(\mu\text{-CX})$ system is very similar. At first this result may seem counterintiutive yet the results simply indicate that the efficient removal of M≡M electron density by the π^* orbitals of CO is so good that a strong σ bond can be formed by CO 5σ orbital donation to the metal. The weaker σ–π synergism of the $W_2(\mu\text{-CNR})$ bonding results in a situation whereby CO and CNR have comparable σ-donor ability in the bridging ligand systems reported here. This is by no means a new concept. In their seminal studies of the transition-metal–isocyanide bond, Fenske and Sarapu found that CO was actually a better σ-donor than $CNCH_3$ based on calculated orbital occupations for $[MnL_6]^+$ (L = CO, $CNCH_3$).[21] Furthermore, Jolly and co-workers have come to a similar conclusion for $Fe(CO)_4(CNR)$ complexes based on elegant He I and X-ray photoelectron spectroscopic studies.[22]

One very important observation revealed by the Mulliken populations of Table IX is that the $2\pi_\parallel$ orbital has a substantially higher occupation than the $2\pi_\perp$ orbital for all CX ligands. Stronger π back-bonding to the $2\pi_\parallel$ orbital occurs because the $2\pi_\parallel$ orbital is involved in a strong σ interaction with the W_2 fragment as compared to the weaker π interaction between the $2\pi_\perp$ and W_2 fragment orbitals. This is illustrated schematically in III. The preference for stronger π back-donation into the $2\pi_\parallel$ orbital is directly responsible for the C–N–R bending to occur parallel to the M–M axis. Equivalent π back-bonding to both 2π orbitals would preclude any preference for C–N–R bending. As shown in Figure 7, bending the isocyanide ligand parallel to the M–M axis stabilizes the $2\pi_\parallel$ orbital due to the decrease in C–N antibonding character in the orbital. As a result, the $2\pi_\parallel$ orbital obtains better orbital energetics (Figure 7) and increased overlap (Table VIII) with W_2 fragment orbitals. Bending the CNR moiety in the $W_2(\mu\text{-CNR})$ compounds results in a dramatic stabilization of the $7b_2$ M–C σ-bonding orbitals, and this is demonstrated for R = H in the correlation diagram in Figure 8 comparing linear and bent $W_2(OH)_6(\mu\text{-CNH})$. The enhanced π-acceptor ability of the $2\pi_\parallel$ orbital of the bent isocyanide ligand is revealed as an increase in the Mulliken populations of the bent CNR ligand (R = H, CH_3) relative to the linear CNR ligand as seen in Table IX.

(21) Sarapu, A. C.; Fenske, R. F. *Inorg. Chem.* **1975**, *14*, 247; *Inorg. Chem.* **1972**, *11*, 3021.

(22) Beach, D. B.; Bertoncello, R.; Granozzi, G.; Jolly, W. L. *Organometallics* **1985**, *4*, 311.

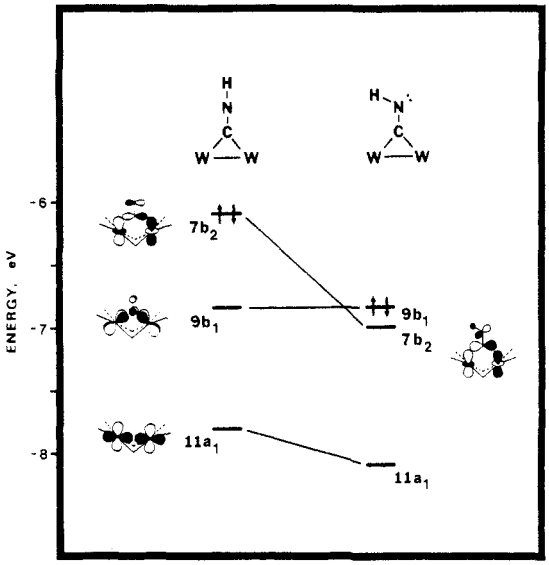

Figure 8. Molecular orbital diagram comparing the primarily metal-localized valence orbitals of linear and bent $W_2(OH)_6(\mu$-CNH).

There is one other phenomenon which occurs upon C–N–R bending which we feel has important consequences to $M_2(\mu$-CNR) bonding. Bending the C–N–R moiety renders the $W_2(\mu$-CNR) molecular plane as the only symmetry element (C_s symmetry). Molecular orbitals are either symmetric (a′) or antisymmetric (a″) with respect to this plane. The 5σ and $1\pi_{\parallel}$ orbitals both have a′ symmetry and mix upon bending. When bridging two transition metals, the nature of this mixing is altered and its magnitude enhanced relative to the free ligand.[23] The result of $5\sigma/1\pi_{\parallel}$ mixing in the $M_2(\mu$-CNR) system is to polarize the 5σ and $1\pi_{\parallel}$ orbitals such that the new hybrids are directed syn and anti with respect to the direction of CNR bending. This polarization phenomenon is more severe for the $1\pi_{\parallel}$ orbital than the 5σ, and the resulting $1\pi_{\parallel}$ hybrid orbital must now be considered as a donor orbital. This situation is very similar to the $5\sigma/1\pi_{\parallel}$ mixing seen in $[W_2(OH)_6(\mu\text{-CO})]_2$.[5] The $5\sigma/1\pi_{\parallel}$ mixing is illustrated schematically for the resulting $1\pi_{\parallel}$ hybrid in IV. The

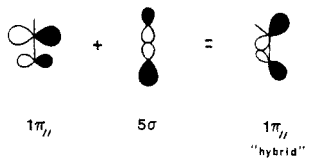

IV

hybrid 5σ and $1\pi_{\parallel}$ donor interactions with $W_2(OH)_6$ produce the 9a′ and 10a′ MO's of bent $W_2(OH)_6(\mu$-CNH), respectively, and contour plots of these orbitals are shown in Figure 9. The 9a′ orbital is predominantly 5σ in character and can be compared to the $7a_1$ orbital plot shown in Figure 6. The result of the new $1\pi_{\parallel}$ donor orbital is to afford a slightly stronger interaction between the isocyanide carbon and metal atom anti to R as shown qualitatively in V. The slightly stronger W(anti)–C in-

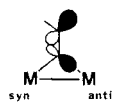

V

(23) The mixing of 5σ and $1\pi_{\parallel}$ orbitals in the $M_2(\mu$-CNR) system found here is very similar to that reported by Howell and co-workers; see ref 15b.

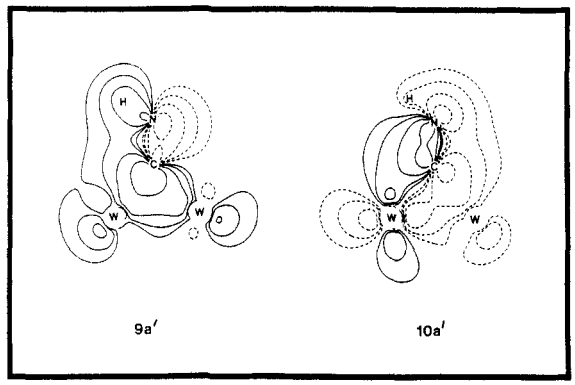

Figure 9. Contour plots of the 9a′ and 10a′ W–C σ-bonding orbitals of $W_2(OH)_6(\mu$-CNH) with a bent CNH moiety. Plots represent a slice taken through the plane containing the $W_2(\mu$-CNH) moiety.

teraction is revealed in the W–C atomic orbital overlap populations which provide a relative measure of syn and anti W–C bond strength. In the linear geometry, both W–C bonds are equivalent with a W–C atomic orbital overlap population of 0.437. Maintaining identical W–C bond lengths and simply bending the C–N–H bond angle to 130° drops the W(syn)–C overlap population slightly to 0.430 and increases the W(anti)–C overlap population to 0.456. It is tempting to suggest that this latter effect manifests itself as an asymmetry in the experimental W–C distances reported here as suggested by Saillard and coworkers.[15b] Unfortunately, although there appears to be such an asymmetry in the W–C bonds, the precision of the W–C distances is not sufficient to make this definitive. However, we belive this trend will be observed whenever sufficiently accurate structural data are to be found.

The Effect of Lewis Base Association. In our studies of $M_2(\mu$-CO)-containing compounds, we demonstrated that Lewis base association resulted in enhanced π back-bonding into the $2\pi_{\parallel}$ orbital of CO.[5] It is not surprising that we find the identical result for the isocyanide analogoues. Although we have only isolated a mono-Lewis base adduct, we have examined the effect of Lewis base association on the model compound $W_2(OH)_6(NH_3)_2(\mu$-CNH) to afford a direct comparison with the carbonyl results. The enhanced π back-bonding is revealed in the Mulliken populations of the canonical orbitals of the CNH ligand in $W_2(\mu$-CNH)L_2 species shown in the bottom of Table IX. A more detailed analysis of the Lewis base interaction with the $M_2(\mu$-CX) moiety has been given in ref 5.

Concluding Remarks

This work shows that the addition of 1 equiv of an aryl or alkyl isocyanide to $W_2(O\text{-}t\text{-}Bu)_6$ leads to the formation of $W_2(O\text{-}t\text{-}Bu)_6(\mu$-CNR) in direct analogy to our previous results on carbonylation reactions. Aryl isocyanide ligands react with $W_2(O\text{-}i\text{-}Pr)_6(py)_2$ to form $W_2(O\text{-}i\text{-}Pr)_6(py)(\mu$-CNR) with the liberation of 1 equiv of pyridine, and this observation is understandable in terms of steric control in the binding of pyridine.

These new molecules afford the unique opportunity to compare carbonyl and isocyanide ligands in identical molecular environments. The ^{13}C NMR chemical shift of the μ-CNR ligand is at slightly higher field, with slightly smaller ^{183}W–^{13}C coupling constants than the μ-CO ligand, consistent with the notion that carbonyl is a stronger π-acid than isocyanide in the $W_2(\mu$-CX)-containing molecules. Nevertheless, the extremely low-field ^{13}C chemical shift of 280 ppm implies substantial carbyne character to the W–C bonds, and the ν(C–N) values of 1530 cm^{-1} are

the lowest of any neutral bridging isocyanide compound in the current literature.[9]

Fenske–Hall calculations suggest that the weakening of the C–N bond upon interaction with the strongly reducing $(W{\equiv}W)^{6+}$ unit can be attributed primarily to the degree of π back-bonding in the $W_2(\mu\text{-CNR})$ moiety. The calculations indicate that carbonyl is a stronger π-acid than isocyanide in the bridging position and a measure of the relative magnitude of π back-bonding has been obtained from the Mulliken populations of the canonical orbitals of the coordinated CO and CNR moieties. Inequivalent π back-bonding to the 2π orbitals of the CNR ligand results in a higher Mulliken population of the $2\pi_{\parallel}$ orbital. Bending the C–N–R moiety enhances the π-acceptor ability of this orbital, and hence a bending parallel to the M–M axis is favored and easily rationalized. In this regard, we note that to the best of our knowledge, all bent, bridging isocyanide ligands are bent parallel to the M–M axis.

Experimental and Computational Procedures

Physical Techniques. ^{1}H NMR spectra were recorded on a Nicolet NT-360 spectrometer at 360 MHz in dry and oxygen-free toluene-d_8 or benzene-d_6. ^{13}C NMR spectra were recorded on a Varian XL-300 spectrometer at 75 MHz in toluene-d_8 solvent and employing $Cr(acac)_3$ as a shiftless relaxation reagent and preaquisition delay times of up to 8 s. All ^{1}H NMR chemical shifts are reported in parts per million relative to the CHD_2 quintet of toluene-d_8 set at δ 2.09 or the ^{1}H impurity in benzene-d_6 set at δ 7.15. All ^{13}C NMR chemical shifts are reported in parts per million relative to the methyl carbon of toluene-d_8 set at δ 20.4.

Infrared spectra were recorded on a Perkin-Elmer 283 spectrophotometer as Nujol mulls between CsI plates. Elemental analyses were performed by Alfred Bernhardt Mikroanalytisches Laboratorium, West Germany.

Synthesis. General procedures and the preparations of $W_2(O\text{-}i\text{-}Pr)_6py_2$ and $W_2(O\text{-}t\text{-}Bu)_6$ have been described.[7] All reactions were carried out under an atmosphere of dry and oxygen-free nitrogen by using standard Schlenk and glovebox techniques. Hexane and toluene were degassed and eluted from activated copper catalyst and molecular sieve columns and then stored over sieves and under nitrogen. *tert*-Butyl isocyanide was purchased from Aldrich, degassed, and stored under nitrogen prior to use. 2,6-Dimethylphenyl isocyanide was purchased from Fluka and was used without further purification. Glassware may be conveniently freed from the isocyanide odor by rinsing with a 1:10 mixture of concentrated hydrochloric acid and methanol.

$W_2(O\text{-}t\text{-}Bu)_6(CNxylyl)$. In a Schlenk reaction vessel equipped with a tight-fitting septum, $W_2(O\text{-}t\text{-}Bu)_6$ (0.25 g, 0.31 mmol) was dissolved in toluene (10 mL) to give a deep red solution. The flask was closed to nitrogen flow and then cooled to 0 °C. Exactly 1 equiv (0.31 mmol in a 0.03 M toluene solution) of 2,6-dimethylphenyl isocyanide was added dropwise to the stirred solution via cannula transfer. This was accompanied by an immediate color change from red to brown. The solution was stirred for 20 min, the volume reduced by one-half, and cooled to −15 °C for 24 h which produced a large mass of small black crystals. The crystals were collected by cannula filtration and dried in vacuo. A second and third crop of crystals was obtained by reducing the volume of the filtrate and cooling [total yield 0.21 g, 72% based on tungsten]. Anal. Calcd for $W_2O_6NC_{33}H_{63}$: C, 42.27; H, 6.77; N, 1.49 Found: C, 40.72; H, 6.47; N, 1.57. Anal. Calcd for one less carbon, $W_2O_6NC_{32}H_{63}$: C, 40.99; H, 6.77; N, 1.49.

^{1}H NMR (−60 °C, toluene-d_8): δ(O-*t*-Bu) 1.24 (18 H, s), 1.58 (36 H, s); $\delta(C_6H_3Me_2)$ 2.73 (6 H, s); δ (p-$C_6H_3Me_2$) 6.77 (1 H, t, $^3J_{HH}$ = 7.2 Hz); δ(o-$C_6H_3Me_2$) 7.44 (2 H, d, $^3J_{HH}$ = 7.2 Hz).

^{1}H NMR (21 °C, toluene-d_8): two isomers seen in relative ratio 7:1. Major isomer: δ(O-*t*-Bu) 1.44 (54 H, s); $\delta(C_6H_3Me_2)$ 2.64 (6 H, s); δ(p-$C_6H_3Me_2$) 6.67 (1 H, t, $^3J_{HH}$ = 7.2 Hz); δ(o-$C_6H_3Me_2$) 7.37 (2 H, d, $^3J_{HH}$ = 7.2 Hz). Minor isomer: δ(O-*t*-Bu) 1.48, 1.52, 1.61 (54 H, singlets); $\delta(C_6H_3Me_2)$ 3.09 (6 H, s); δ(o-$C_6H_3Me_2$) 7.11 (2 H, d, $^3J_{HH}$ = 7.2 Hz).

^{13}C{^{1}H} NMR (22 °C, toluene-d_8): two isomers observed. Major isomer: δ(*C*Nxylyl) 275.5. Minor isomer: δ(*C*Nxylyl) 268.6.

IR (cm^{-1}); ν_{CN} 1531 s; other bands, 1235 m, 1170 s, 970 s, 960 s, 940 s, 922 s, 875 m, 780 m, 770 m, 755 m, 672 w, 565 m, 535 m, 455 m.

$W_2(O\text{-}t\text{-}Bu)_6(CN\text{-}t\text{-}Bu)$. In a Schlenk reaction vessel $W_2(O\text{-}t\text{-}Bu)_6$ (0.50 g, 0.62 mmol) was dissolved in toluene (20 mL) to give a deep red solution. The solution was cooled to 0 °C, and exactly 1 equiv (0.62 mmol) of *t*-BuNC was added via a microliter syringe with stirring. The solution immediately turned from red to dark green. The green solution was stirred at 0 °C for 1 h and the volume reduced by three-fourths. The $W_2(O\text{-}t\text{-}Bu)_6(CN\text{-}t\text{-}Bu)$ molecule is very soluble in hydrocarbon solvents. In order to obtain crystals, several small pellets of solid CO_2 were placed in the bottom of a beaker, and the Schlenk reaction vessel placed on top and cooled to −15 °C. This produced many large green crystals after 3 days. The crystals were collected by cannula filtration and dried in vacuo. A second crop of crystals was obtained by reducing the volume of the filtrate to about 4 mL and seeding with one small crystal of $W_2(O\text{-}t\text{-}Bu)_6(CN\text{-}t\text{-}Bu)$ previously obtained [total yield 0.34 g, 58% based on tungsten].

^{1}H NMR (−95 °C, toluene-d_8): δ(O-*t*-Bu) 1.49 (18 H, s) 1.64 (36 H, s); δ(CN-*t*-Bu) 2.00 (9 H, s). ^{1}H NMR (21 °C, toluene-d_8) three very broad singlets at δ 1.58, 1.59, and 1.63.

^{13}C{^{1}H} NMR (22 °C, toluene-d_8): δ(μ-*C*N-*t*-Bu) 281.3 ($^1J_{^{183}W-^{13}C}$ = 136.5 Hz); $\delta(C(CH_3)_3)$ 82.8, 79.2, 68.7; $\delta(C(CH_3)_3)$ 33.3, 32.7.

IR (cm^{-1}): ν_{CN} 1528 m (br); other bands, 1335 m, 1280 s, 1025 w, 1005 m, 960 s, 925 m, 910 m, 780 m, 685 m, 560 m, 475 m, 360 m.

$W_2(O\text{-}i\text{-}Pr)_6(CNxylyl)(py)$. In a Schlenk reaction vessel $W_2(O\text{-}i\text{-}Pr)_6(py)_2$ (0.46 g, 0.52 mmol) was dissolved in toluene (15 mL) to give a blood-red solution. The solution was cooled to 0 °C. Exactly 1 equiv (0.52 mmol in a 0.05 M toluene solution) of 2,6-dimethylphenyl isocyanide was added dropwise to the stirring solution via cannula transfer. The color appeared to darken to brown. The solution was stirred at 0 °C for 1 h and the volume reduced by one-half and cooled to −15 °C. After 2 days a very oily residue was present. The solvent was removed, the resulting solids were dried in vacuo and then redissolved in hexane, and the volume was reduced slightly and cooled to −15 °C. After 24 h, many large brown crystals were present. The crystals were collected by cannula filtration and dried in vacuo. A second crop of crystals was obtained by reducing the volume of the filtrate and cooling [total yield 0.29 g, 60% based on tungsten].

^{1}H NMR (21 °C, toluene-d_8): two isomers present in 7:1 ratio. Major isomer: $\delta(OCHMe_2)$ 1.91 (36 H, d, $^3J_{HH}$ = 6.1 Hz); δ-($OCHMe_2$) 4.95 (6 H, br); $\delta(C_6H_3Me_2)$ 2.67 (6 H, s), δ (p-$C_6H_3Me_2$) 6.79 (1 H, t, $^3J_{HH}$ = 7.6 Hz); δ(o-$C_6H_3Me_2$) 7.33 (2 H, d, $^3J_{HH}$ = 7.6 Hz); $\delta(C_5NH_5)$ 9.07 (5 H, br).

IR (cm^{-1}): ν_{CN} 1535 m (br); other bands, 1600 w, 1325 w, 1170 m, 1115 s, 980 s, 845 m, 755 w, 750 w, 690 w, 600 m.

Computational Procedures. We have employed the model systems $W_2(OH)_6(\mu\text{-CNR})$, where R = H or CH_3, and $W_2(OH)_6(NH_3)_2(\mu\text{-CNH})$ to investigate the nature of $W_2(\mu\text{-CNR})$ bonding and the effects of Lewis base association on these systems. The coordinates for $W_2(OH)_6(\mu\text{-CNR})$ were idealized to C_{2v} point symmetry (linear CNR, R = H, CH_3), but otherwise bond distances and angles were taken from the crystal structure of $W_2(O\text{-}t\text{-}Bu)_6(CNxylyl)$ reported here. The W–W, W–C, and C–N distances used were 2.52, 2.00, and 1.25 Å, respectively. The W to μ_2-O and terminal O distances were averaged to 2.09 and 1.87 Å, respectively. An O–H distance of 0.96 Å was used. For the CNR ligands the N–H and N–CH_3 distances were 1.01 and 1.45 Å, respectively. For the CH_3 group, the C–H bond length and H–C–H angle were assigned values of 1.00 Å and 109.5°, respectively. For the Lewis base adduct $W_2(OH)_6(NH_3)_2(CNH)$, W–N and N–H distances of 2.28 and 1.01 Å and an H–N–H angle of 107° were used.

Molecular orbital calculations were performed by using the Fenske–Hall method which has been discussed in detail elsewhere[16] and its applications reviewed.[24] The Fenske–Hall method is an approximate Hartree–Fock–Roothaan SCF–LCAO procedure, and the final results depend only upon the chosen atomic basis set and internuclear distances. SCF calculations were performed in the atomic basis on the CNR and $W_2(OH)_6$ fragments and on the $W_2(OH)_6(CNR)$ complexes (R = H, CH_3). To

(24) (a) Fenske, R. F. *Prog. Inorg. Chem.* **1976**, *21*, 179. (b) Fenske, R. F. *Pure Appl. Chem.* **1971**, *27*, 61.

Table X. Summary of Crystal Data

	I[a]	II[b]
empirical formula	$W_2C_{33}H_{63}NO_6$	$W_2C_{32}H_{56}N_2O_6$
color of cryst	black	black
cryst dimens, mm	0.12 × 0.12 × 0.20	0.18 × 0.16 × 0.19
space group	*Pbca*	$P2_1/n$
cell dimens		
T, °C	−158	−155
a, Å	18.768 (5)	9.880 (3)
b, Å	23.566 (8)	19.071 (6)
c, Å	17.311 (6)	19.903 (7)
β, deg		104.05 (1)
Z (molecules/cell)	8	4
V, Å^3	7656.17	3638.12
D(calcd), g/cm^3	1.627	1.703
wavelength, Å	0.710 69	0.710 69
mol wt	937.51	932.50
linear abs coeff, cm^{-1}	61.715	64.941
detector to sample dist, cm	22.5	22.5
sample to source dist, cm	23.5	23.5
av *ω* scan width at half-height, deg	0.25	0.25
scan speed, deg/min	4.0	4.0
scan width, deg + dispersn	2.0	2.0
individual bgd, s	8	8
aperture size, mm	3.0 × 4.0	3.0 × 4.0
2*θ* range, deg	6–45	6–45
total no. of reflctns collected	5770	6097
no. of unique intensities	5041	4796
no. with $F > 0.0$	4305	
no. with $F > 2.33\sigma(F)$	2720	
no. with $F > 3.00\sigma(F)$		3190
R(*F*)	0.0577	0.0661
$R_w(F)$	0.0548	0.0599
good of fit for the last cycle	0.989	1.138
maximum Δ/σ for the last cycle	0.05	0.05

[a] I = W_2(O-*t*-Bu)$_6$(CNxylyl). [b] II = W_2(O-*i*-Pr)$_6$(py)(CNxylyl).

aid in the interpretation of the results, the converged wave functions were transformed into a basis consisting of the canonical orbitals of the isolated CNR and $W_2(OH)_6$ fragments. All calculations were obtained at the Indiana University Computational Chemistry Center by using a VAX 11/780 computer system. Contour plots were generated on a TALARIS 800 laser printer with solid lines representing positive density contours and dashed lines representing negative density contours.

All atomic wave functions were generated by a best fit to Herman–Skillman atomic calculations by using the method of Bursten, Jensen, and Fenske.[25] Contracted double-ζ representations were used for the W 5d AO's as well as C, O, and N 2p AO's. Basis function for the W atom were derived for a +1 oxidation state with the 6s and 6p exponents fixed at 1.8. An exponent of 1.16 was used for the H 1s atomic orbital since that value gives the minimum energy for methane.[26]

Crystallographic Studies. General operating procedures and listing of programs have been previously reported.[27] A summary of crystal data is given in Table X for the two compounds examined in this work.

W_2(O-*t*-Bu)$_6$(CNxylyl). A suitable crystal was located and transferred to the goniostat by using standard inert atmosphere handling techniques employed by the Indiana University Molecular Structure Center and cooled to −158 °C for characterization and data collection. It was necessary to examine numerous crystals before one was obtained that was not badly split. As a result, the size was somewhat less than ideal.

A systematic search of a limited hemisphere of reciprocal space located a set of diffraction maxima with orthorhombic symmetry and systematic extinctions corresponding to the unique space group *Pbca*. Data were collected in the usual manner by using a continuous *θ*/2*θ* scan technique. Data were reduced in the usual manner. The structure was solved by a combination of direct methods (MULTAN78) and Fourier techniques and refined by full-matrix least squares. Although some of the hydrogen atom positions were visible in a difference Fourier phased on the non-hydrogen parameters, the low number of observed data precluded their attempted refinement. The positions of all hydrogens were calculated and placed in fixed idealized positions (d(C–H) = 0.95 Å) for the final cycles. The hydrogen atoms were assigned thermal parameters of 1 + B_{iso} of the carbon atom to which they were bound. In the final least squares, only the tungsten atoms were allowed to refine anisotropically, with hydrogens fixed and all other atoms isotropic.

A final difference Fourier was essentially featureless, with the largest peak being 0.50 e/Å^3, except for two peaks of intensity 1.2 and 1.4 e/Å^3, one at each metal position.

W_2(O-*i*-Pr)$_6$(py)(CNxylyl). A suitable crystal was located and transferred to the goniostat by using standard inert atmosphere handling techniques employed by the Indiana University Molecular Structure Center and cooled to −155 °C for characterization and data collection.

A systematic search of a limited hemisphere of reciprocal space located a set of diffraction maxima with symmetry and systematic absences corresponding to the monoclinic space group $P2_1/n$. Subsequent solution and refinement of the structure confirmed this choice.

Data were collected in the usual manner by using a continuous *θ*/2*θ* scan with fixed backgrounds. Data were reduced to a unique set of intensities and associated sigmas in the usual manner. The structure was solved by a combination of direct methods (MULTAN78) and Fourier techniques. Many of the hydrogen atom positions were visible in a difference Fourier phased on the non-hydrogen atoms. Positions were calculated for all hydrogens assuming idealized geometry (with d(C–H) = 0.95), and they were included as fixed atom contributors in the final cycles.

A final difference Fourier was essentially featureless, with the largest peak being 1.3 e/Å^3 located adjacent to W(1). A *ψ* scan of several reflections near *χ* = 90° indicated that no absorption correction was necessary, with a maximum deviation of ca. 8%.

Acknowledgment. We thank the National Science Foundation for financial support and Dr. C. D. Ontiveros for obtaining ^{13}C NMR spectra. D.L.C. is the recipient of the 1985–1986 General Electric Foundation Fellowship. We also thank the National Science Foundation for departmental supported instruments (VAX 11/780, CHE-83-09446 and CHE-84-05851; Nicolet 360 NMR, CHE-81-05004).

Registry No. 1, 108151-02-6; 2, 108169-99-9; W_2(O-*t*-Bu)$_6$, 57125-20-9; W_2(O-*t*-Bu)6(CN-*t*-Bu), 108151-03-7; W_2(O-*i*-Pr)$_6$(Py)$_2$, 70178-75-5; $W_5(OH)_6(\mu$-CNH), 108151-04-8; $W_2(OH)_6(\mu$-CNCH$_3$), 108151-05-9; $W_2(OH)_6(NH_3)_2$(M-CNH), 108151-06-0; $W_2(OH)_6(\mu$-CO), 103671-08-5; C≡O, 630-08-0; C≡NH, 6914-07-4; C≡N-CH$_3$, 593-75-9; W, 7440-33-7.

Supplementary Material Available: Tables of anisotropic thermal parameters, complete listings of bond distances and angles, and VERSORT drawings and stereoviews for W_2(O-*t*-Bu)$_6$(CNxylyl) and W_2(O-*i*-Pr)$_6$(py)(CNxylyl) (15 pages); F_o and F_c values for W_2(O-*t*-Bu)$_6$(CNxylyl) and W_2(O-*i*-Pr)$_6$(py)(CNxylyl) (17 pages). Ordering information is given on any current masthead page.

(25) Bursten, B. E.; Jensen, J. R.; Fenske, R. F. *J. Chem. Phys.* **1978**, *68*, 3320.
(26) Hehre, W. J.; Steward, R. F.; Pople, J. A. *J. Chem. Phys.* **1969**, *51*, 2657.
(27) Chisholm, M. H.; Folting, K.; Huffman, J. C.; Kirkpatrick, C. C. *Inorg. Chem.* **1984**, *23*, 1021.